Partial Discharge Charge Estimation In Gas-Insulated Substations Using Electric and Magnetic Antennas

Mier Escurra, Christian; Mor, Armando Rodrigo

DOI
10.1109/ICD53806.2022.9863499

Publication date
2022

Document Version
Final published version

Published in
Proceedings of the 2022 IEEE 4th International Conference on Dielectrics (ICD)

Partial Discharge Charge Estimation In Gas-Insulated Substations Using Electric and Magnetic Antennas

Christian Mier Escurra
Delft University of Technology
Delft, Netherlands
C.MierEscurra@tudelft.nl

Armando Rodrigo Mor
Universitat Politècnica de València
Valencia, Spain
arrodmor@ite.upv.es

2022 IEEE 4th International Conference on Dielectrics (ICD) | 978-1-6654-1833-1/22/$31.00 ©2022 IEEE | DOI: 10.1109/ICD53806.2022.9863499

***Abstract*— Partial discharges (PD) measurements provide an estimation of the severity of the insulation degradation; additionally, it is used as a unit of standardization. Up to now, only the IEC 62478 briefly mentions partial discharge measurements using electromagnetic sensors in gas-insulated substations (GIS). The IEC60270 standard provides a method for PD charge measurement when the test object approximates to a lumped element; PD in SF_6 are in the range of nanosecond, and given the GIS length, it behaves as a transmission line. This work compares different sensors (commercially available and developed by the authors) used for measuring PD charge magnitude in GIS. The sensors' sensitivity, time resolution, and charge estimation accuracy are tested in a full-scale 420 kV GIS. A nanosecond rise time pulse was connected to the GIS through a transition cone to provide a good PD representation. The pulse was measured by electric and magnetic sensors installed in mounting holes located in different sections of the GIS, and a directional coupler was used as a reference to the injected pulse. This work demonstrates that the charge magnitude can be extracted using different sensors, harmonizing the reading from different measuring systems. The results show the possibility of a standardized method for on-line PD measurements and routine and after-installation tests.**

Keywords—Partial discharge, gas-insulated substation, magnetic antenna, electric antenna, charge estimation.

I. Introduction

It is known from the literature that partial discharges (PD) measurements are an accepted method for insulation diagnosis [1]. IEC 60270 [2] provides a guide for conventional PD charge estimation methods; for unconventional methods, there is no recommendation since according to [2]: *do not directly quantify the apparent charge of the PD current pulses*. On the other hand, [3] and [4] demonstrate that unconventional electric detectors, dealing with conducted signals, can estimate the charge. Studies presented in [5] and [6] conclude that a PD charge, in principle, can be estimated in a gas-insulated substation (GIS) when the sensor measures the transverse electromagnetic (TEM) mode.

A new sensor, consisting of a magnetic antenna, is proposed for measuring PD in GIS [7]. This sensor and the voltage double integral method [8] allow the PD charge magnitude estimation [8]. Additionally, the voltage double integral method was demonstrated in [4] for electric antennas (also known as UHF sensors or capacitive couplers) with a bandwidth (BW) below the transverse electric (TE) mode.

Reference [9] presented a test bench for characterization of PD sensors in GIS: this test bench was fully matched to 50 Ω using transition cones. In this research, the sensors are analyzed in a full-scale 420 kV GIS: since the GIS is not matched, a different test setup is proposed. First, the sensors and the test setup are described; and second, the results are discussed for the different antennas and GIS locations: sensors sensitivity, resolution, and charge estimation errors. This investigation shows the possibility of measuring PD charges in GIS with unconventional electromagnetic methods.

"This project 19ENG02 FutureEnergy has received funding from the EMPIR programme co-financed by the Participating States and from the European Union's Horizon 2020 research and innovation programme"

II. Methods

A. PD Sensors

Two different sensors were tested for this research: a magnetic loop antenna and an electric antenna. The magnetic loop antenna consists of a shielded loop constructed of RG174A-U coaxial cable; the sensor has a ferrite choke for common-mode currents mitigation (a detailed description is found in [9] and [10]). The electric antenna is a commercial capacitive coupler, a picture and the dimensions are shown in Fig. 1. The sensors are dimensioned to fit in the GIS mounting holes; therefore, the dimensions and frequency responses differ from those presented in [9] and [10].

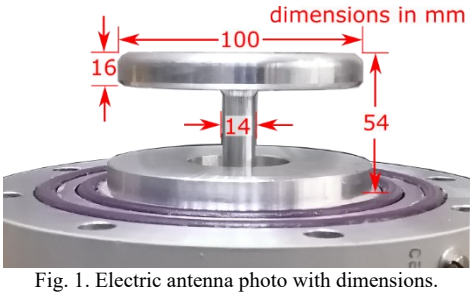

Fig. 1. Electric antenna photo with dimensions.

B. Test setup

The test setup shown in Fig. 2 is proposed to demonstrate that the charge magnitude of a PD pulse can be measured with different sensors in a full-scale GIS. The test setup consists of a pulse generator, reference measurement, sensors, and instrumentation. A nanosecond pulse calibrator was connected to the GIS through a directional coupler (DIRC) and a transition cone. The propagated pulse was measured with antennas installed in different mounting holes in the GIS; at the output of the antennas, an amplifier and a filter were connected. The DIRC is connected to the GIS by a BNC connector; since the GIS has a diameter more than 100 times bigger, a transition cone was used. Fig. 3 shows a picture of the outer transition

cone connected to the GIS enclosure; a second cone was installed for the inner conductor.

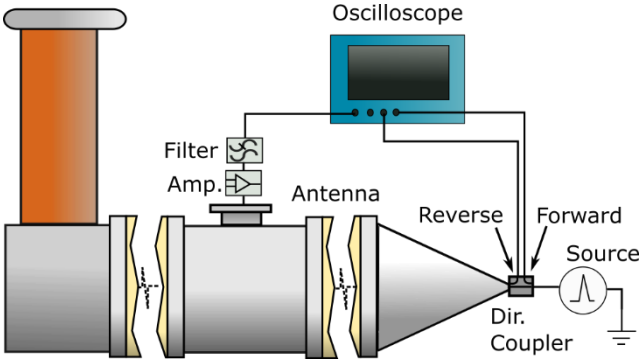

Fig. 2. Test setup for pulse measurements using PD antennas.

Fig. 3. Picture of the transition cone in the test setup.

The transmitted pulse to the GIS is measured using the directional coupler ZFBDC20-62HP+. The GIS at the injection position has a different characteristic impedance than the pulse generator, transmitting a different pulse. The transmitted charge is the sum of the incident and reflected charges, as shown in (1) and (2): where V, V^+ and V^- are the transmitted, incident and reflected pulses, respectively; G is the DIRC's gain; and Q, Q^+ and Q^- are the transmitted, incident and reflected charges, respectively. The method is validated according to Fig. 4: a pulse is connected to the DIRC input; then an oscilloscope in parallel with a 50 Ω resistor is connected to the DIRC's output, representing the change of impedance in the GIS. Fig. 6 a) shows the coupled forward and reverse pulses (divided by the 0.1 direction coupler gain), and b) shows the transmitted pulse to the oscilloscope compared with the addition of the directional coupler outputs. The charge transmitted to the oscilloscope is compared with the subtraction of the coupled forward and backward charges (Fig. 6 b)), giving a 0.8% error.

$$V(t) = V_0^{+}(t) + V_0^{-}(t) \tag{1}$$

$$Q \approx \frac{1}{G}\int_0^{\infty} V_0^{+} dt + \frac{1}{G}\int_0^{\infty} V_0^{-} dt \approx Q^{+} + Q^{-} \tag{2}$$

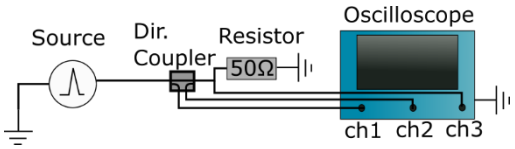

Fig. 4. Test to verify the reference charge calculation using a DIRC.

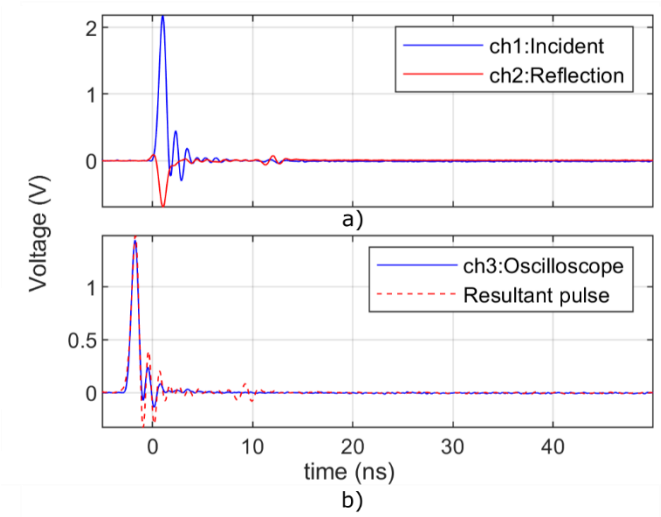

Fig. 5. a) Incident and reflected measured pulses in the DIRC, and b) transmitted pulse compared with the resultant DIRC outputs.

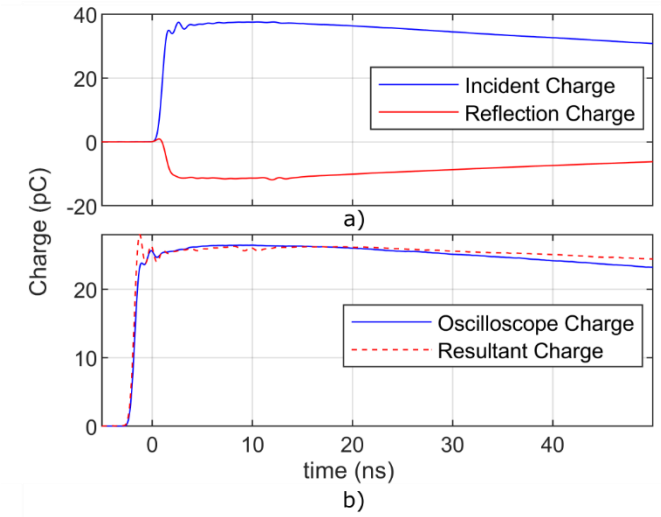

Fig. 6. a) DIRC output's estimated charges and b) transmitted charge compared with resultant DIRC estimated charge.

Fig. 7 shows the injection point and antennas positions in the GIS. Each position is affected differently by the discontinuities: position number 1 is 1.6 m from the pulse source, and it is closely located in between two spacers; it is known that the geometry and materials of the spacer change the characteristic impedance [11]; position 2 is at 6.1 m from the source, and it is far from any discontinuity; position 3 is 18 m away from the source, and it is immediately after a T section (2/3 attenuation [12]).

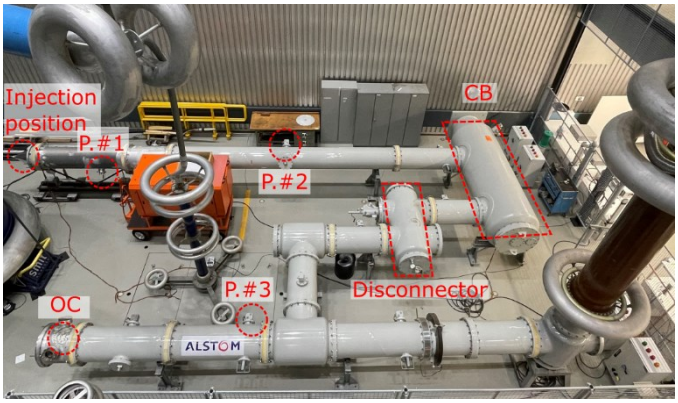

Fig. 7. GIS top view showing the injection point, antennas' position, and GIS discontinuities.

C. Charge Estimation Method

The magnetic and electric antennas have a narrow and derivative response [9], allowing the use of the voltage double integral charge estimation method [13]. This method consists of the double integral of the output voltage, divided over a constant (3); to avoid the accumulation of noise and pulse reflections, the integration time is limited to the second zero crossing of the voltage pulse (t_0). The constant k is obtained with (4) by the calibration procedure presented in [4]. The directional coupler has a broad frequency response (1-700 MHz), allowing the charge calculation through the current pulse integration [6]. The charge estimation is validated with the reference and antennas charges.

$$q(t) \approx \frac{1}{k}\int_0^{t_0}\int_0^{t_0} V_0(t)dt \tag{3}$$

$$lim\left|\frac{H(\omega)}{\omega}\right|_{\omega\to 0} \approx k \;\; when\; \omega \neq 0 \tag{4}$$

III. Results

Fig. 8 a) shows the measured reference pulses in the directional coupler, and b) to d) shows the magnetic and electric antennas measured pulses from position 1-3, respectively. The time integration limits are marked with a black cross. Table 1 shows the reference, the magnetic and electric antenna charges magnitudes in different positions. The last two rows show the charge estimation errors of the antennas.

Table 2 shows the time and space resolution for each measurement. The time resolution of the pulse is the time from the beginning of the pulse to the second zero crossing (crosses in Fig. 8). The spatial resolution is calculated using the time resolution and the average propagation speed: the speed is estimated by dividing the distance between positions 3 and 1 over the time delay between them, giving a speed of 28.6 cm/ns.

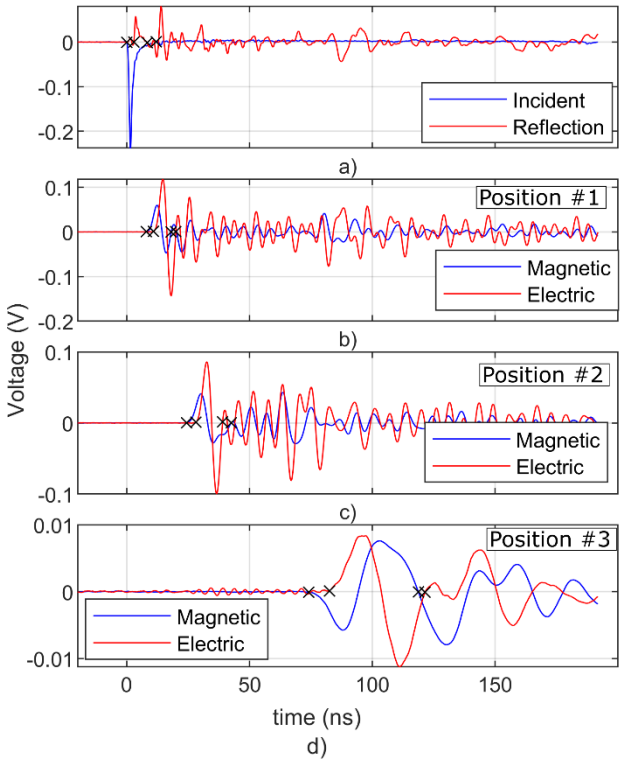

Fig. 8. a) Incident and reflection coupled pulses in the DIRC. b) – d) Magnetic and electric antennas' pulses measurements from positions 1 to 3. The time integration limits are marked with a black cross.

Table 1. Charge estimation and charge error for the magnetic and electric antennas in different positions.

Ref. Charge	74.4 pC		
Antenna	Position #1	Position #2	Position #3
Mag. Charge	56.6 pC	80.1 pC	50.4 pC
Elec. Charge	59.5 pC	56.9 pC	60.7 pC
Mag. Error	-24%	7.6%	-32%
Elec. Error	-20%	-24%	-18%

Table 2. Time and space resolution for the magnetic and electric antennas in different positions.

Resolution	Position #1	Position #2	Position #3
Mag. Time	10.1 ns	18.2 ns	44.6 ns
Elec. Time	9.12 ns	10.9 ns	38.9 ns
Mag. Space	2.88 m	5.22 m	12.8 m
Elec. Space	2.61 m	3.11 m	11.1 m

IV. Discussion

From previous results, the following can be concluded: The DIRC's coupled reverse output measured multiple reflections (Fig. 8 a); however, the reference charge is calculated using the incident pulse minus the first reflected pulse, which is the reflection in the transition from the calibrator to the GIS. The subsequent pulses are discarded since they are the reflections that come from the different discontinuities in the GIS.

The electric antenna shows a better sensitivity over the magnetic antenna because of its higher calibration constant and

cutoff frequency. In position three, the high frequency is completely attenuated, giving a similar sensitivity for both antennas: the electric sensor pulse peak is reduced by a factor of 14. There is low attenuation between positions 1 and 2, meaning that the attenuation mainly comes from the circuit breaker and disconnector; hence, sensors must be installed between these discontinuities to improve the GIS coverage.

The distance heavily attenuates the signals' high frequencies; the pulse duration increases from 9 ns in position 1 to 39 ns in position 3 (4 times increase). A low resolution encourages the overlapping of reflections; this is seen in Fig. 8 d): since the pulse length is 12.8 m, it is affected by the reflections at the bushing and the bottom open circuit.

Both antennas show similar charge estimation capabilities with a maximum error of around 25%. The magnetic antenna in position two exhibits a lower error, attributed to a constructive reflection overlapping. In position three, the magnetic antenna error is increased: the signal is distorted by reflections overlapping. Overall, the charge estimation is affected by multiple factors: low sensor resolution (reflection overlapping), calibration constants approximation and charge estimation approximations; however, both antennas show a similar charge value, demonstrating a harmonization between them. Regarding the charge estimation and pulse resolution, it is difficult to conclude which antenna performs better; further analysis is needed to study the behavior in noisy environments.

V. Conclusions

The investigation has shown the possibility to estimate the PD charge magnitude by using magnetic and electric antennas in the very high-frequency range. A coaxial cone was used to provide a smooth transition of the input pulse to the rest of the GIS, giving a neat representation of the propagation in the TEM mode. The proposed method paves the way for a standardized method for on-line PD measurements and routine and after-installation tests, and sets the principles of harmonization of partial discharge charge measurements using electric and magnetic antennas in GIS.

VI. References

[1] Working Group D1.33, "Guidelines for unconventional Partial Discharge Measurements," *Cigre,* vol. D1, no. 444, p. 58, 2010.

[2] British Standard, "IEC 60270," British standard, 2001.

[3] A. Cavallini, G. C. Montanari and M. Tozzi, "PD apparent charge estimation and calibration: A critical review," *IEEE Transactions on Dielectrics and Electrical Insulation,* vol. 17, no. 1, pp. 198-205, 2010.

[4] C. Mier, A. Rodrigo, L. Castro and P. Vaessen, "Magnetic and Electric Antenna Calibration for Partial Discharge Charge Estimation in Gas Insulated Substations," *in press.*

[5] G. Behrmann and Z. Tanasoc, "UHF PD signal transmission in GIS: Effects of 90 bends and L-shaped CIGRE step 1 test section.," p. 9, 2019.

[6] A. Rodrigo, P. Morshuis and J. Smit, "Comparison of Charge Estimation Methods in Partial Discharge Cable Measurements," *IEEE Transactions on Dielectrics and Electrical Insulation.,* vol. 22, no. 2, p. 8, 2015.

[7] A. Rodrigo, F. A. Muñoz and L. C. Castro, "A Novel Antenna for Partial Discharge Measurements in GIS Based on Magnetic Field Detection," *Sensors,* vol. 19, no. 858, p. 17, 2018.

[8] A. Rodrigo, L. C. Castro and F. A. Muñoz, "A magnetic loop antenna for partial discharge measurements on GIS," *Elsevier International Journal of Electrical Power & Energy Systems,* vol. 115, no. 105514, p. 6, 2019.

[9] C. Escurra and A. Mor, "Test Bench and Frequency Response of a Magnetic Antenna used in GIS PD Measurements," in *IEEE EIC*, Denver, 2021.

[10] C. Escurra, A. Mor and P. Vaessen, "Design and Characterization of a Magnetic Loop Antenna for Partial Discharge Measurements in Gas Insulated Substations," *IEEE sensors Journal,* vol. 21, no. 17, pp. 18618-18625, 2021.

[11] H. Imagawa, K. Emoto, H. Murase, H. Koyama, R. Tsuge, S. Maruyama and T. Sakakibara, "PD signal propagation characteristics in GIS and its location system by frequency components comparison," *IEEE Transactions on Power Delivery,* vol. 16, no. 4, pp. 564-570, 2001.

[12] M. Hikita, S. Ohtsuka, T. Hoshino, S. Maruyama, G. Ueta and S. Okabe, "Propagation Properties of PD-induced Electromagnetic Wave in GIS Model Tank with T Branch Structure," *IEEE Transactions on Dielectrics and Electrical Insulation,* vol. 18, no. 1, pp. 256-263, 2011.

[13] A. Rodrigo, F. Muñoz and C. C. Luis, "Principles of Charge Estimation Methods Using High'Frequency Current Transformers Sensors in Partial Discharge Measurements," *Sensors,* vol. 20, no. 2520, p. 16, 2020.